Wireless Pers Commun (2017) 93:833–852
DOI 10.1007/s11277-014-2231-z

Transmitted Power Formulation for the Optimization of Spectrum Aggregation in LTE-A over 800 MHz and 2 GHz Frequency Bands

Jessica Acevedo Flores · Daniel Robalo · Fernando J. Velez

Published online: 25 December 2014

Abstract This work starts by proposing a formulation to calculate the transmitter power needed to cover cells of different sizes, whilst maintaining the average signal to interference-plus-noise ratio constant, and near the maximum, for two Long Term Evolution (LTE) systems operating over non-contiguous frequency bands, 800 MHz and 2 GHz, with an integrated common radio resource management (iCRRM) entity. In the context of spectrum aggregation (SA), iCRRM is able to switch users between the two LTE-Advanced scenarios to facilitate the best user allocation and maximize the total network throughput in these LTE systems. We address a formulation based on the computation of the average received power and average co-channel interference in cellular topologies with frequency reuse pattern $K = 3$, keeping the presence of coverage holes insignificant, whilst considering the COST-231 Hata path loss model. We have verified how the normalized power increases as the cell radius increases. The objective of applying this formulation in the dimensioning process is to save power for the shortest coverage distances. It has been found that without SA the maximum average cell throughput is observed in the presence of 80 simultaneous users within the cell (40 for each LTE system, operating in different frequency bands). We have considered traced-based video sessions with a (video) bit rate of 128 kbps. In this scenario, through extensive simulations cell average supported throughput of approximately 6,800, 8,500 and 9,500 kbps have been obtained for the cases without SA (considering the sum of the 800 MHz and 2 GHz systems capacities), with a simple CRRM and with iCRRM, respectively. It was also found that when the peak throughput is achieved with 80 users, the average cell packet loss ratio without SA, with CRRM and iCRRM present values of 22, 11 and 7 %. The average cell delay with both CRRM and iCRRM entities is 22 ms, whereas without SA is equal to 32 ms. Finally, the cost/revenue tradeoff is analysed from the operator/service provider's point of view, whose

J. A. Flores · D. Robalo · F. J. Velez (✉)
Instituto de Telecomunicações, DEM, Universidade da Beira Interior, Covilhã, Portugal
e-mail: jacevedo@cip.org.pe

D. Robalo
e-mail: drobalo@lx.it.pt

F. J. Velez
e-mail: fjv@ubi.pt

main goal is obtain the maximum profit from his business. It was found that CRRM increases the total profit in percentage, compared to a simple allocation, without SA. Nevertheless, the profit growth with iCRRM is even larger, from 253 to 296 % for $R = 1{,}000$ m and a price of 0.010 €/MByte. Therefore, our proposal for SA is convenient not only in terms of technical features and QoS, as loss and delay have been obtained within a range of reasonable values, but also in terms of economic aspects.

Keywords Long Term Evolution Advanced · Radio resource management · Signal to interference-plus-noise ratio · Spectrum aggregation · Wireless systems

1 Introduction

Most of the spectrum bands suitable for terrestrial wireless communication have already been allocated by the regulatory agencies to existing licensees, which has led to a spectrum scarcity problem. Dynamic spectrum access (DSA) techniques are promising to enable spectrum aggregation (SA) with intra-operator multiband scheduling [1]. DSA takes advantage of the non-uniform geographic and temporal distribution of traffic and interferers within a network, improving the efficiency of idle and underutilised radio frequency bands through sharing, coexistence and aggregation.

The main motivations in introducing SA (also referred as carrier aggregation, CA, for Long-Term Evolution-Advanced, LTE-A, in Release 10 [2]) were the support of high data rates, efficient utilization of fragmented spectrum, and support of heterogeneous network deployments by means of cross-carrier scheduling. In the case of CA, multiple LTE carriers, referred to as a component carrier (CC), from an RF point-of-view, and each with a bandwidth up to 20 MHz, can be transmitted in parallel to/from the same terminal, thereby allowing for an overall wider bandwidth and correspondingly higher per-link data rates. In the context of CA, three types of aggregation are possible: intraband aggregation, contiguous and non-contiguous CCs, and interband aggregation. LTE-A [2] includes bandwidth extension via SA to support 1 Gbps peak rates in downlink and 500 Mbps in the uplink over a wireless connection considering bandwidths of 100 MHz.

Radio resource management (RRM) plays an important role in the optimization of wireless system design, due to the scheduling algorithm which decides among packets that are ready for transmission. Based on the scheduling algorithm which allocates CCs resource blocks to users, as well as the traffic characteristics of the multiplexed flows, the optimization of radio and network planning is tuned, and certain quality of service (QoS) requirements can be achieved. Common RRM (CRRM) refers to the set of functions that are devoted to ensure an efficient and coordinated use of the available radio resources in heterogeneous networks scenarios. A non-contiguous SA (from an upper layer point of view) and an integrated CRRM (iCRRM) entity for multiband scheduling are proposed in [3], where SA and CRRM functionalities are handled simultaneously in an LTE-A scenario. The proposed resource allocation (RA) assigns the user packets to the available radio resources, i.e., CCs, in order to satisfy user requirements based on integer programming optimization, or even suitability based optimization, and ensures efficient packet transport to maximize spectral efficiency.

The first step for the adaptation of the iCRRM proposal in [3] to LTE-A is the formulation for the average signal to interference-plus noise ratio (SINR) that allows for setting the basic limits for the dependence of the transmitter power in the context of SA with multiband scheduling on the coverage distance in LTE systems. Moreover, a revised and updated version of the iCRRM entity optimization at system level is also proposed in this work. The

enhancement in the obtained average supported cell throughput is evaluated and analysed through extensive simulations. The final contribution from this work is the analysis of the cost/revenue tradeoff that results from the use of SA.

The remaining of this work is organised as follows: Sect. 2 provides an overview of related research on CCs allocation schemes. Section 3 addresses aspects of supported throughput enhancement through SA employing multiband scheduling. Section 4 presents the topology and the average SINR formulation, which further allows for obtaining the normalized transmitter powers. Section 5 describes the updated iCRRM multiband scheduler and profit function, LTE-A scenario simulations and achieved average supported cell supported throughput. Section 6 describes the cost/revenue model and analyses the obtained optimization results. Finally, Sect. 7 addresses the main conclusions from this research.

2 Related Work

The selection of CC, to assign multiple CCs to users, is the new RRM functionality introduced in LTE-Advanced. For CC selection, UEs information such as the QoS requirements and terminal capability can be exploited as well as the measured information including the overall traffic level, the traffic load per CCs, and the channel quality information from UEs [4]. Furthermore, the optimization of CCs assignment and allocation to each UE according to the CC characteristic, e.g., channel quality and load, remains one of the key issues for CA of radio resource management. In the majority of the current work on radio frequency resource allocation for CA only the downlink is addressed, as most of nowadays applications require higher throughputs in the downlink.

Following the available research in the literature, three main methods for balancing the load across CCs may be derived. For the first, the *Random Selection* (RS) scheme, CCs are randomly chosen by the eNB for each UE. As a result, it can provide balanced load across CCs. However, at each instant, the load across CCs may not be balanced and the system may suffer from reduced spectrum utilization [4]. The second scheme, called *Circular Selection* (CS), selects CCs circularly for the data traffic. Compared to RS, this scheme improves throughput and coverages performance due to better balancing of traffic load over multiple CCs [4]. Finally, the third scheme, the *Least Load* (LL) rule, allocates user packets to each CC according to the current trafc load of CCs. As so, enhanced load balancing across the CCs can be expected from this scheme in comparison to the previous ones that do not consider the system state information [4].

Nevertheless, the optimization of inter-band CC selection should not only address traffic load, but also the radio channel characteristics, e.g., received signal strength. In this context, the iCRRM entity proposed in this paper addresses such radio channel quality information, as well as QoS requirements, in terms of loss.

3 Throughput Improvement Through Spectrum Aggregation with a Multiband Scheduler

SA with intra-operator multiband scheduling [2] can contribute to alleviate the spectrum scarcity problem. An ideal scheduling scheme combined with SA is required to facilitate the communication using non-contiguous spectrum bands, with improved average error ratio and delay performance. We assess a multiband CRRM (MB-CRRM) entity, proposed in [3], to schedule users between the 800 MHz and 2 GHz frequency bands in a single operator scenario,

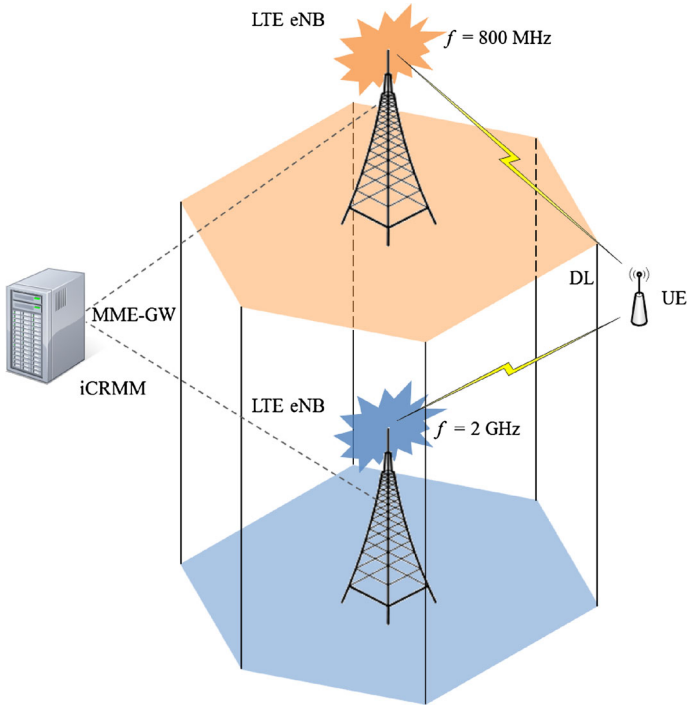

Fig. 1 LTE network scenario considering two frequency bands

under a constant average SINR, considering the LTE Simulator from [5]. Our study is similar to the one from [3], where the authors implemented iCRRM, i.e., considered multiband scheduler able to schedule users between the 2 and 5 GHz frequency bands. However, the RAT considered in this previous work was the High-Speed Downlink Packet Access (HSDPA) and not LTE-A. In their results, shown in Sect. 5, Fig. 11, from [3], an almost constant gain near 30 % was obtained with their proposed optimal solution compared to a system where users are initially allocated into one of the two bands through multiband scheduling, and later are not able to switch users between the bands, during the sessions.

As to achieving results from simulations requires to have an adequate balance between the values of SINR from LTE systems operating at the two bands, we propose a formulation to obtain the average SINR that facilitates having comparable coverage range between the two co-located addressed systems. It is still important to remember that the formulation from [3] considers the unlicensed shared 5 GHz band, while this work addresses two licensed bands.

Figure 1 shows the LTE-A system scenario considering the main network nodes, i.e., eNodeB (eNB), user equipment (UE), and Mobility Management Entity/Gateway (MME/GW).

3.1 Path Loss Model

The radio channel follows the widely used ITU radio propagation COST-231 Hata model [6] and [7]. We have selected this path loss model for our formulation because of its accurateness and simplicity. For medium size cities, the model is given by the following equation:

Table 1 Parameters for LTE DL budget for a data rate of 1 Mbps and an omnidirectional antenna

Transmitter–Node B		
a) Max. T_X power (dBm)	50	
b) TX antenna gain (dBi)	3–3.5	For 800 MHz and 2 GHz respectively
c) Body loss (dB)	2	
d) EIRP (dBm)	**51–51.5**	$= a + b - c$
f) Receiver noise floor (dBm)	−99	$= -174 + 10 \cdot \log_{10}(BW) + e$
g) SINR (dB)	−10	From simulations
h) Receiver sensitivity (dBm)	−109	$= f + g$
i) Interference margin (dB)	3	
j) Cable loss (dB)	1	
k) RX antenna gain (dBi)	0	
l) Fast fade margin (dB)	0	
m) Maximum path loss (dBm)	**156–156.5**	$= d - h - i - j + k - l$

$$L_{[\mathrm{dB}]} = 40 \cdot (1 - 4 \times 10^{-3} \cdot D_{hb[\mathrm{m}]}) \log_{10}(R_{[\mathrm{km}]}) - 18 \cdot \log_{10}(D_{hb[\mathrm{m}]}) + 21 \cdot \log_{10}(f_{[\mathrm{MHz}]}) + 80 \quad (1)$$

for urban and suburban scenarios, outside the high rise core, where the buildings are of nearly uniform height. In (1), R is the separation between the base station (BS) or eNB and the UE, f is the carrier frequency, and D_{hb} is the BS antenna height, measured from the average rooftop level.

Considering two carrier frequencies, 800 MHz and 2 GHz, $D_{hb} = 15$ m and a UE antenna of 1.5 m, one considers the following path loss model:

$$L_{800\,\mathrm{MHz}[\mathrm{dB}]} = 119.16 + 37.6 \cdot \log_{10}(d_{[\mathrm{km}]})$$
$$L_{2\,\mathrm{GHz}[\mathrm{dB}]} = 128.1 + 37.6 \cdot \log_{10}(d_{[\mathrm{km}]}) \quad (2)$$

3.2 LTE Downlink Budget

Let us consider that LTE DL uses orthogonal frequency division multiple access (OFDMA), the frame duration is fixed at 10 ms, the frame is divided into subframes of 1 ms duration. A subframe consists of two slots of 0.5 ms duration. The BS schedules transmissions every 1 ms, which is known as transmission time interval (TTI), and resource blocks are formed from the subcarriers for allocation for the DL. In order to obtain results comparable to the ones from [3], the selected bandwidth (BW) is the intermediate value of 5 MHz, which guarantees high bit rates, depending on the type of modulation and coding. Using a BW of 5 MHz and single stream, 25 resource blocks and 300 subcarriers are required (plus another one for control usage), each one of which has a 15 kHz spacing. Table 1 presents the design parameters, considering real values from a commercial omnidirectional antenna [8] and taking the values from [9] into account. The lines in bold represent quantities that result from sums and differences from previous variables in the table, as represented in the third column.

4 Topology and Average SINR Analysis

The SA gain is evaluated for several inter-cell distances with a frequency reuse pattern K, equal to three. A similar evaluation was carried out in [3], with a frequency reuse pattern of one, then the average SINR was obtained following a method similar to the one described in [10]. As K increases the co-channel interference in the system decreases. In order to have comparable results, SA needs to be analysed at constant average SINR, which is achieved only by tuning the BSs transmitter power.

4.1 SINR at a Given Position

According to [10] (Chap. 12), for a topology with a UE in a given position $(y, 0)$ and for $K = 3$, the inter-cell BSs distance is $3R$, as it is shown in Fig. 2.

Given a BS transmitter power, P_{Tx}, the SINR of a UE at position (x, y) can be expressed by:

$$SINR(P_{Tx}, x, y) = \frac{P_{ow}(P_{Tx}, x, y)}{(1-\alpha) \cdot P_{ow}(P_{Tx}, x, y) + P_{nh}(P_{Tx}, x, y) + P_{noise}} \tag{3}$$

where P_{ow} is the power received from the own cell, α is the orthogonality factor according to [9], P_{nh} is the total amount of interfering power coming from the neighbour cells (six cells in the case of hexagonal cell deployment model), and the thermal noise power, P_{noise}, which is a function of the thermal noise received through an ideal matched filter for each modulation, and also depends on the UE noise figure (typical of 7–9 dB for LTE). Then, P_{noise} is expressed as:

$$P_{noise} = -174 + 10 \cdot \log_{10}(BW) + NF \tag{4}$$

where BW ($BW = 5$ MHz) is the bandwidth and NF is the noise figure ($NF = 8$ dB, as shown in Table 1).

According to [2], for HSPA, $(1-\alpha) \cdot P_{ow}(P_{Tx}, x, y)$ with $\alpha \in [0, 1]$, denotes the average channel multipath orthogonality factor, i.e., the fraction of the total output power

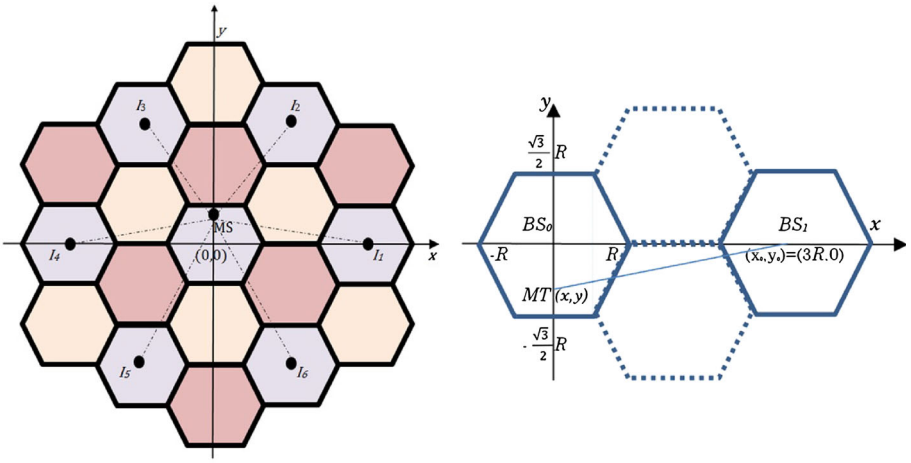

Fig. 2 Topology considered in our formulation with $K = 3$ (*left-hand side*), and the inter and intra cell interference for an LTE network (*right-hand side*)

that is experienced as intra-cell interference as the channels from the same cell are no longer perfectly orthogonal. Furthermore, for HSDPA, $\alpha < 0.9$ is often assumed, while for WCDMA, values in the range $\in$ [0.5, 0.9] are recommended. The authors from [11] mention that, in LTE, even though non-idealities may result in non-negligible own-signal interference (e.g., inter-symbol interference due to multipath power exceeding cyclic prefix length, inter-carrier interference due to Doppler spread, transmit signal waveform distortion due to transmitter non-linearities), the orthogonality factor is often assumed as unitary, for the sake of simplicity.

At the 800 MHz and 2 GHz frequency bands the power received from the own cell, P_{ow}, can be represented as:

$$P_{ow-800\,\mathrm{MHz}}(P_{Tx}, x, y) = P_{Tx} G_{Tx} G_{Rx} 10^{-\frac{119.6+37.6\cdot\log\sqrt{y^2+x^2}}{10}} \tag{5}$$

$$P_{ow-2\,\mathrm{GHz}}(P_{Tx}, x, y) = P_{Tx} G_{Tx} G_{Rx} 10^{-\frac{128.1+37.6\cdot\log\sqrt{y^2+x^2}}{10}} \tag{6}$$

where G_{Tx} and G_{Rx} are the transmitter and receiver gains, respectively. $P_{nh}(P_{Tx}, x, y)$ is the interference power received by a UE from the ring of six cells, with BS-distance $D = \sqrt{(x_0 + y_0)} = \sqrt{(3R + 0)} = \sqrt{3K}R = 3R$, for reuse pattern $K = 3$, as shown in Fig. 2. Such interference power is given by:

$$P_{nh}(P_{Tx}, x, y) = \sum_{i=1}^{6} I_i(P_{Tx}, x, y) \quad \text{with,} \quad I_1 = I_4,\ I_2 = I_3,\ I_5 = I_6 \tag{7}$$

where $I_i(P_{Tx}, x, y) = P_{Tx} G_{Tx} G_{Rx} 10^{-\frac{PL(x,y)^i}{10}}$ and i represents the cell from which the interference comes from, as also defined in [3].

At the 800 MHz frequency band, the following functions stand for the path loss, PL, that corresponds to the interference from cell i:

$$\begin{aligned} PL(x, y)^{1,4} &= 119.6 + 37.6 \cdot \log\sqrt{\left(\frac{3}{2}R\right)^2 + \left(\frac{3\sqrt{3}}{2}R - y\right)^2} \\ PL(x, y)^{2,3} &= 119.6 + 37.6 \cdot \log\sqrt{\left(\frac{3}{2}R\right)^2 + \left(\frac{3\sqrt{3}R}{2} + y\right)^2} \\ PL(x, y)^{5,6} &= 119.6 + 37.6 \cdot \log\sqrt{(3R)^2 + (y^2)} \end{aligned} \tag{8}$$

Figure 3 shows the variation of the SINR as a function of the MS-BS distance, d ($0 \leq d \leq R$), with P_{Tx} constant and equal to a selected value of 1 dBW. According to the specifications, transmitter antenna gains are $G_{Tx\,800\,\mathrm{MHz}} = 3$ dBi, and $G_{Tx\,2\,\mathrm{GHz}} = 3.5$ dBi, and receiver gain is $G_{Rx} = 0$ dBi. Results are presented in Fig. 3 for cell radii of 300 and 1,500 m.

4.2 Average SINR in the Cell

The average SINR within a cell is the SINR measured by a UE with uniform probability density function for its deployment over the cell area. It depends on the cell radius, R, and on the BS transmitter power, P_{Tx}, as follows:

$$\overline{SINR}(R, P_{Tx}) = \frac{\overline{P}_{ow}(R, P_{Tx})}{(1-\alpha)\overline{P}_{ow}(R, P_{Tx}) + \overline{P}_{nh}(R, P_{Tx}) + P_{noise}} \tag{9}$$

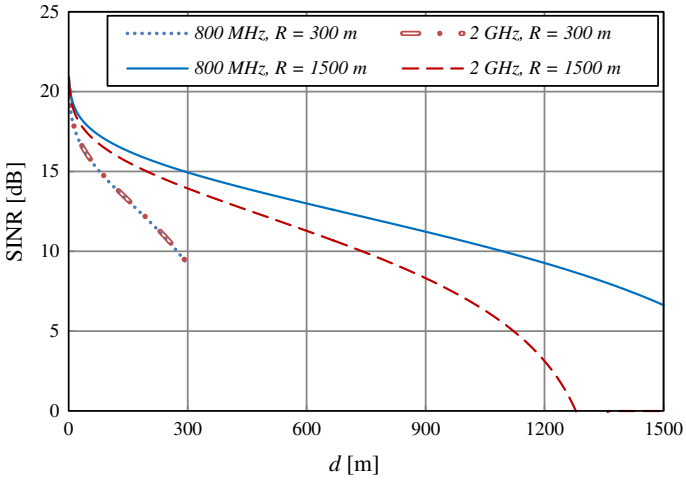

Fig. 3 SINR as a function of the UE-BS distance for two cell radii ($R \in \{300, 1{,}500\}$ m) and $P_{Tx} = 1$ dBW

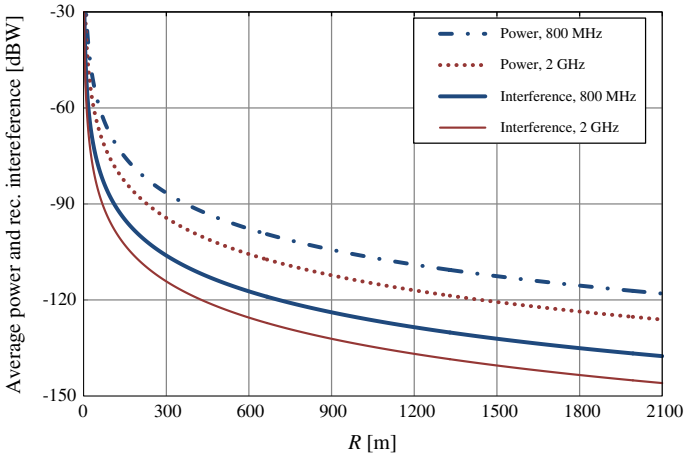

Fig. 4 Average power and interference (dBW) within a cell as a function of the inter-cell distance (m) with $P_{Tx} = 1$ dBW and $\alpha = 1$

The average interference generated by a neighbour cell can be calculated by integrating each fraction of the interfering power over the area of the affected cell. Figure 2 shows one cell affected by interference in the origin of the coordinates and one interfering cell, at (x_0, y_0). By integrating over the hexagonal cell area, the average level of the received power from a neighbour cell, $\bar{I}$, may be calculated as:

$$\bar{I}(R, P_{Tx}) = \int_y \int_x f_I(P_{Tx}, x, y) dx dy = \int_y \int_x \frac{P_{Tx} G_{Tx} G_{Rx}}{A_{cell}} PL(x, y) dx dy \qquad (10)$$

where A_{cell} is the total affected cell area. As the surrounding interfering neighbours are all at the same distance, $3R$, $\overline{P}_{nh}(R, P_{Tx}) = 6 \cdot \bar{I}(R, P_{Tx})$.

Figure 4 shows the variation of the average received power and interference with the cell radius for $\alpha = 1$. Details for the calculation of the average interference can be found in

[10]. $\overline{P}_{ow}(P_{Tx,x,y})$ is the average signal power within a cell and it is constant for the same frequency model, no matter what value of K is used.

The calculation of the average signal power within a cell is also shown in [3], following a similar approach as the one for the average interference calculation, with a different integrand function, which due to the geometry of the problem, has a simpler expression. Equations (11–14) show the results of our integrations as a function of the cell radius, R, for both frequency bands:

$$P_{ow-800\,\mathrm{MHz}}(P_{Tx},x,y) = P_{Tx}G_{Tx}G_{Rx}\cdot 10^{-\sum_{r=1}^{3}\int_{\Gamma^r_{x,y}}\frac{119.6+37.6\cdot\log\sqrt{y^2+x^2}}{10\cdot A_{cell}}} \tag{11}$$

$$P_{nh-800\,\mathrm{MHz}}(P_{Tx},x,y) = P_{Tx}G_{Tx}G_{Rx}\cdot 10^{-\sum_{r=1}^{3}\int_{\Gamma^r_{x,y}}\frac{119.6+37.6\cdot\log\sqrt{y^2+x^2}}{10\cdot A_{cellnh}}} \tag{12}$$

$$P_{ow-2\,\mathrm{GHz}}(P_{Tx},x,y) = P_{Tx}G_{Tx}G_{Rx}\cdot 10^{-\sum_{r=1}^{3}\int_{\Gamma^r_{x,y}}\frac{128.1+37.6\cdot\log\sqrt{y^2+x^2}}{10\cdot A_{cell}}} \tag{13}$$

$$P_{nh-2\,\mathrm{GHz}}(P_{Tx},x,y) = P_{Tx}G_{Tx}G_{Rx}\cdot 10^{-\sum_{r=1}^{3}\int_{\Gamma^r_{x,y}}\frac{128.1+37.6\cdot\log\sqrt{y^2+x^2}}{10\cdot A_{cellnh}}} \tag{14}$$

where $A_{cellnh}=\frac{3\sqrt{R^2}}{2}$ is the area for a hexagonal cell, $A_{cell}=\frac{3\sqrt{R^2}}{2}-4Fr^2$ is the total integration area to calculate the signal/power and own cell interference, and Fr is the Fraunhofer distance (its value is different for each frequency band and depends on antenna characteristics), similar to the calculation in [3].

By determining the exponent in (11) and (12), we obtain (15) and (16), respectively:

$$\begin{aligned}\sum_{r=1}^{3}\int_{\Gamma^r_{x,y}}\frac{119.6+37.6\cdot\log_{10}\sqrt{y^2+x^2}}{10A_{cell}} &= \left(12Fr^2\frac{9\sqrt{3}}{2}+\frac{3\pi R^2}{2}-4Fr^2\right.\\ &\times\operatorname{arccot}\left(\frac{2Fr}{\sqrt{3}R}\right)-4Fr^2\cdot\arctan\left(\frac{2Fr}{\sqrt{3}R}\right)-2Fr^2\cdot\ln(4)-8Fr^2\cdot\ln(Fr)\\ &\left.+3\sqrt{3}R^2\cdot\ln(R)\right)\cdot\left(\frac{37.6}{4\ln(10)}\right)+(A_{cell}(119.6-(37.6\cdot\log(1000))))\left(\frac{10}{A_{cell}}\right)\end{aligned} \tag{15}$$

$$\begin{aligned}\sum_{r=1}^{3}\int_{\Gamma^r_{x,y}}\frac{128.6+37.6\cdot\log_{10}\sqrt{y^2+x^2}}{10A_{cellnh}} &= \left(\frac{1}{4}R^2\left(-18\sqrt{3}-4\pi\right.\right.\\ &+2\operatorname{arccot}\left(\frac{5}{\sqrt{3}}\right)-2\operatorname{arccot}\left(\frac{7}{\sqrt{3}}\right)+76\operatorname{arccot}\left(\frac{19}{\sqrt{3}}\right)-24\operatorname{arccot}(2\sqrt{3})\\ &+48\operatorname{arccot}\left(\frac{2}{\sqrt{3}}\right)+144\operatorname{arccot}\left(\frac{5}{\sqrt{3}}\right)-144\operatorname{arccot}\left(\frac{7}{\sqrt{3}}\right)+64\sqrt{3}\ln(2)\\ &-15\sqrt{3}\ln(13)-\sqrt{3}\ln(5488)-3\sqrt{3}\ln(16807)+2\sqrt{3}\ln(62748517)\\ &\left.\left.+10\sqrt{3}\ln(R)+2\sqrt{3}\ln(64R)\right)\right)+\left(\frac{37.6}{\ln(10)}\right)+(A_{cell}(128.6\\ &-(37.6\cdot\log(1000))))\left(\frac{10}{A_{cell}}\right)\end{aligned} \tag{16}$$

Figure 5 shows a comparison of the average SINR for different values of the transmitter power, $P_{Tx}=-10$, 1 and 10 dBW, considering $\alpha=1$. As it can be seen, at 800 MHz for $P_{Tx}=10$ dBW, the average SINR reaches higher values and it is almost constant for the considered range of distances. Besides, at 2 GHz, for $P_{Tx}=-10$ dBW, the average SINR starts to decrease for relatively small cell radius (300 m). For every value of P_{Tx}, the average

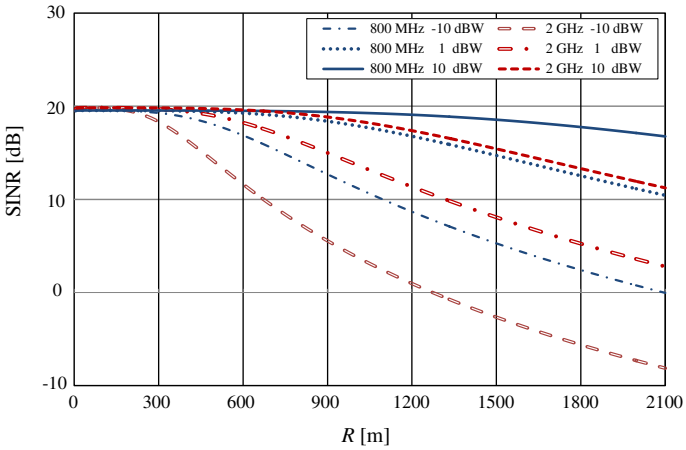

Fig. 5 Average SINR (dB) as a function of the cell radius (m) for three different values of P_{Tx} (−10, 1 and 10 dBW) and $\alpha = 1$

Table 2 Values for the normalized transmitter power $P_{Tx[dBW]}$, for the 800 MHz and 2 GHz bands

V(%)	Freq. Bands (MHz)	Radius (m)						
		300	600	900	1,200	1,500	1,800	2,100
1	800	−3.20	8.00	14.55	19.20	22.80	25.75	28.24
	2,000	6.07	17.38	24.00	28.70	32.34	35.32	37.84
5	800	−10.32	0.88	7.43	12.08	15.68	18.63	21.12
	2,000	1.23	12.55	19.17	23.87	27.51	30.49	33.00
10	800	−13.98	−2.78	3.77	8.42	12.03	14.97	17.46
	2,000	−2.38	8.94	15.56	20.26	23.90	26.88	29.39

SINR at 2 GHz is more affected by the variation of the cell radius and decreases faster than at 800 MHz, especially for low values of the transmitter power.

4.3 Normalization Procedure for the Transmitter Power

The goal of the average SINR analysis is to determine a set of transmitter powers, P_{Tx}, to be considered in system level simulations, in order to have a constant average SINR all over the cell, for all the cell radii, whilst saving power for the shortest coverage distances.

Figure 5 shows the average SINR in both frequency bands with different BS transmitter powers and $\alpha = 1$. It achieves the maximum values of 19.55 and 19.84 dB, for the 800 MHz and 2 GHz frequency bands, respectively. To calculate the normalized P_{Tx}, required in both bands (to maintain such an average SINR constant), we took $\overline{SINR}_{max,f} - V$, where V is the percentage of variation; Table 2 shows the results for the required normalized transmitter powers, P_{Tx}, with variation V equal to 1, 5 and 10 %. Figure 6 shows that, as the cell radius increases, the transmitter power required to keep the envisaged average SINR constant increases as well.

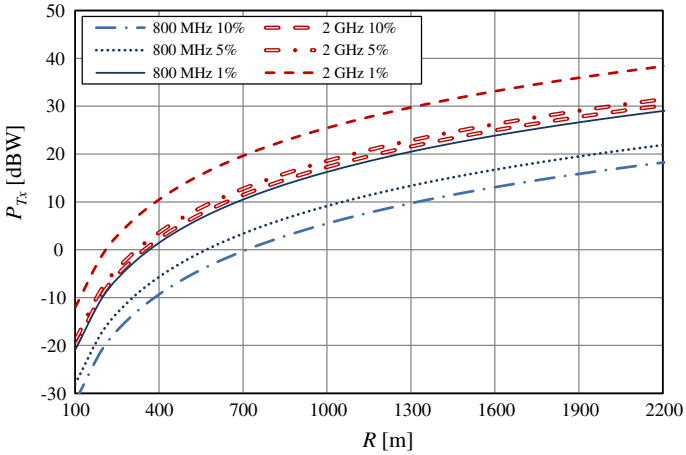

Fig. 6 Normalized P_{Tx} required to achieve a constant average SINR (dB), near the maximum, as a function of the cell radius at 800 MHz and 2 GHz for $\alpha = 1$

5 Analysis of the Supported System Throughput

5.1 General MultiBand Scheduling

Similarly to the analysis from [3], in order to maximize the total video throughput of the operator, SA scheduling is obtained with an optimized General MultiBand Scheduling (GMBS) algorithm. The GMBS problem can be solved with Integer Programming (IP). Its Profit Function (PF) is defined considering the ratio between the rate available on the single DL channel and the requested rate by the service flow. The PF is expressed as follows:

$$(PF) \quad \sum_{b=1}^{m} \sum_{u=1}^{n} W_{bu} x_{bu} \tag{17}$$

where x_{bu} is the allocation variable and the normalized metric W_{bu} is given by:

$$W_{bu} = \frac{[1 - BER(CQI_{bu})] \cdot R(CQI_{bu})}{S_{rate}} \tag{18}$$

where S_{rate} is the NRTV service rate, $BER(CQI_{bu})$ is the average Bit Error Rate (BER) occurred in the previous DL channel transmissions for user u on band b according to the supported Modulation and Coding Scheme, MCS, (0 in the case no transmissions has ever occurred), and $R(CQI_{bu})$ is the DL channel throughput for user u on band b, as a function of the MCS. The allocation variable x_{bu} reflects the band allocation per user and is a Boolean value, $x_{bu} \in \{0, 1\}$, to indicate in which band the user is allocated to.

In the considered scenario, users are deployed over the cell with a uniform spatial distribution, within the range of the cell, R, and it is assumed that user can access multiple frequencies, i.e., UEs have multiple transceivers. However, in the context of this research, the GMBS problem also presents the following constraints:

1. Allocation Constraint (AC): it is considered that each user can be allocated only to a single frequency band at a the time:

$$(AC) \quad \sum_{b=1}^{m} x_{bu} \leq 1, \qquad x_{bu} \in \{0, 1\} \quad \forall\, user\, u$$

2. Bandwidth Constraint (BC): the total number of users on each band is upper bounded by the maximum normalized load that can be handled in the band, $L_b^{max} \in [0, 1]$:

$$(BC) \sum_{u=1}^{n} \frac{S_{rate} \cdot (1 + R_{Tx} \cdot BER(CQI_{bu}))}{R(CQI_{bu})} \cdot x_{bu} \leq L_b^{max} \quad \forall\, band\, b$$

where the first term is the requested service data rate for user u, including the packet loss, normalized with the maximum data rate that the network can offer to the user u on band b which is $R(CQI_{bu})$. BC accounts for the user traffic requirement, DL capacity and overhead caused by packets lost.

Finally, the performance of the SA user allocation is assessed by using the total Service Throughput (ST) which is given by the total number of bits that have been transmitted and correctly received by all the users in the cell:

$$\mathrm{ST}_{[bps]} = \frac{b_{serv} \cdot p}{k \cdot T} \tag{19}$$

where $b_{serv} \cdot p$ is the number of bits received in a given period p, T is the transmit time interval, and $k \cdot T$ is the total simulation time.

5.2 Simulation Scenario

Simulations have been performed by considering the set of cell radii, R, between 300 and 2,200 m with a 100 m increment for the overlapping 800 MHz and 2 GHz bands coverage, as shown in Fig. 1. In this system, each of the two frequency bands is managed separately. Traced-based video sessions, characterised in [5], have been addressed in our simulations. The traced-based application sends packets based on realistic video trace files. Moreover, a video bit rate of 128 kbps and the Modified Largest Weight Delay First (M-LWDF) scheduler [5] have been considered in the system level simulations, as well as the values for the normalised transmitter power from Table 2. 3GPP does not provide any particular suggestion for the scheduling algorithms to be considered in LTE/LTE-A. However, the selected scheduler should satisfy QoS requirements of all users. Considering that M-LWDFs main goal is to prioritize real-time flows with the highest delay for their head of line (HOL) packets and the best channel conditions, and as it offers optimum throughput performance for video applications, it was selected as the scheduler scheme in these simulations. Moreover, for comparison purposes, we also implemented a simple CRRM entity that schedules users on the 2 GHz frequency band until L_{max} is reached. Beyond this capacity threshold the remaining users are allocated in the 800 MHz band.

5.3 Results

The following results represent, in each case, the average of five simulations performed with different initial seeds. The analysis of the results shows that without employing a CRRM entity/SA, one achieves approximately the same behaviour for the network capacity in both frequency bands in the range of the considered cell radii. Figure 7 presents results for the throughput as a function of the number of users obtained with $R = 1{,}000$ m at the 800 MHz and 2 GHz frequency bands. The 95 % confidence intervals are represented for each value considered for the number of users. Figure 8 shows the supported average throughput versus

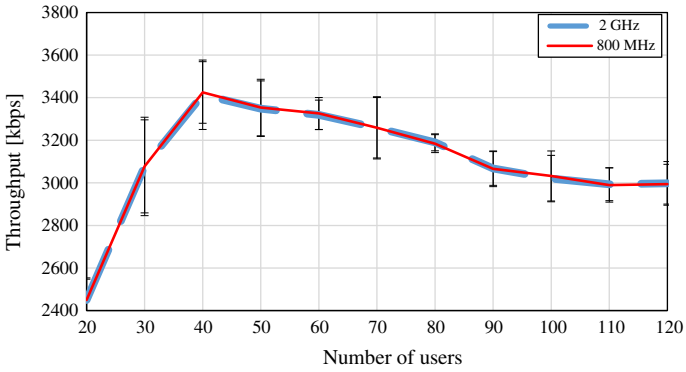

Fig. 7 Average throughput versus number of users for different cell radii, in the absence of CRRM and iCRRM at 800 MHz and 2 GHz, with $R = 1{,}000$ m

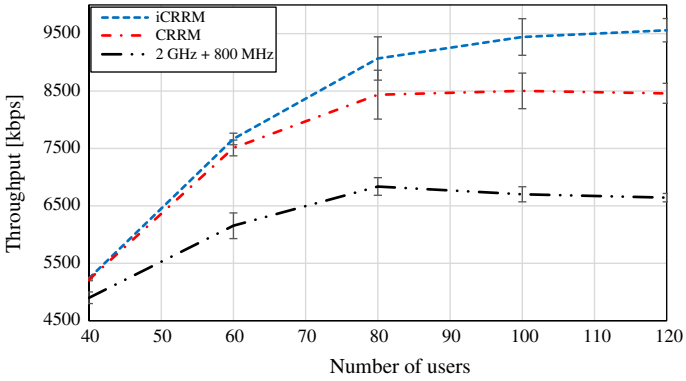

Fig. 8 Average throughput versus number of users for different cell radii, in the presence of CRRM and iCRRM at 800 MHz and 2 GHz, with $R = 1{,}000$ m

the number of users obtained by employing both iCRRM and CRRM against the sum of both frequency bands without SA, and also $R = 1{,}000$ m. Figure 9 shows the average supported cell throughput as a function of the cell radius when 80 users are supported for all considered scenarios, i.e., with iCRRM, CRRM as well as the sum from the capacity for both frequency bands simultaneously.

From all the considered above, it is clear that both SA enabling entities (CRRM and iCRRM) provide superior throughput than the one obtained by only accumulating the capacity of both frequency bands without proper multiband scheduling. When adding forty 800 MHz users with other forty 2 GHz users ($40 + 40 = 80$ users) the maximum average capacity is approximately 6,800 kbps, whereas by employing the CRRM and iCRRM throughput of 8,500 and 9,500 kbps are obtained, respectively. When comparing the average throughput as a function of the cell radii for 80 users, i.e., the number of users that corresponds to the maximum achievable supported throughput without a proper SA implementation optimization, it is still clear that both CRRM and iCRRM entities provide a substantial capacity gain.

Additionally, it is worthwhile to mention that we also addressed the influence of the optimization within the SA entity in terms of average cell packet loss ratio (PLR) and delay. Without SA, when the peak throughput is reached with 80 users, the PLR is approximately

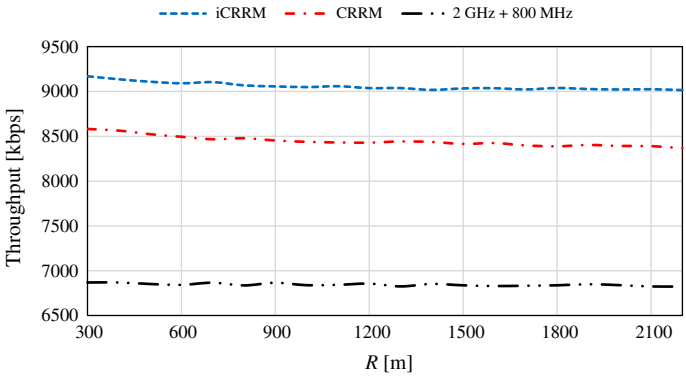

Fig. 9 Comparison of the average throughput as a function of cell radius, R, for 80 users

22 %. The introduction of the CRRM reduces the PLR to 11 % while the use of iCRRM corresponds to a PLR of only 7 %. In terms of delay, without a proper management of spectrum resources and the same number of users, the delay reaches 32 ms. However, the use of both CRRM and iCRRM corresponds to a average cell delay of approximately 22 ms, i.e., 10 ms reduction.

6 Cost/Revenue Optimization

From the economic point of view, the different entities from cellular systems, such as subscribers, network operators, service providers, regulators, and equipment vendors [12], should be taken into account. In this research, we consider operators/service providers point of view, whose main goal is to obtain the maximum profit from his business, i.e., to increase revenue, decreasing costs as much as possible.

In this paper, costs and revenues are analysed on an annual basis, although project duration of 5 years is assumed. Moreover, our analysis is under the assumption of a null discount rate. Nevertheless, this section does not intend to perform a complete economic study, but our aim is simply to present initial contributions to facilitate cellular planning optimization. Appropriate enhancements would be required, in order to perform a complete economic analysis based on discounted cash flows (e.g., to compute the net present value).

From a cellular planning and RRM perspective, the objective of the operator is to determine an optimal operating point that maximizes the expected revenue. Examples of major decisions affecting this include the type of technology to be used, the size of the cell, and the number of radio resources in use in each cell. It is therefore important to identify the main components of system costs and revenues, in particular those that allow a direct relationship to either the maximum cell coverage distance or the reuse pattern.

As it is explained in [12], the cost per unit area is given by:

$$C_{[€/\text{km}^2]} = C_{fi[€/\text{km}^2]} + C_{b[€/\text{cell}]} N_{[\text{cell}/\text{km}^2]} \tag{20}$$

where C_{fi} is the fixed term of the costs (e.g., licensing and spectrum auctions or fees), and C_b is the cost per BS assuming that only one transceiver is used per cell/sector, which corresponds to the installation costs of BSs including the cost of obtaining cell sites, the normal backhaul, and the cost of hardware and core equipment common to all.

The number of cells per unit area is given by:

$$N_{[\text{cell/km}^2]} = \frac{2}{3\sqrt{3}R^2} \tag{21}$$

where R represents the cell radius. Then the total cost per BS, considering every element in the infrastructure, is given by:

$$C_{b[€/\text{cell}]} = \frac{C_{BS} + C_{bh} + C_{inst}}{N_{year}} + C_{M\&O} \tag{22}$$

where N_{year} is the projects lifetime, C_{BS} is the cost of the BS, C_{bh} is the cost for the normal backhaul, C_{inst} is the cost of the installation of the BS, and $C_{M\&O}$ is the cost of operation and maintenance.

Assuming an LTE system in Portugal with the following values for the costs, we consider that C_{BS} is the resulting of summing 20,000 € for both 800 MHz and 2 GHz frequency bands, and also taking into account the C_{BSsite} = 7,000 €, C_{bh} = 5,000 €, C_{inst} = 2,500 € for the radio installation, plus 20,000 € for the total infrastructure (site acquisition, site design and site construction), and $C_{M\&O}$ = 1,500 € per year of operation, considering preventive and corrective infrastructure maintenance, first-line maintenance and rental costs.

The period of time assumed here is $N_{year} = 5$, and $C_{BS} = C_{BS,800\,\text{MHz}} + C_{BS\,2\,\text{GHz}} - C_{BSsite}$ = 33,000 € (the price of the BS site tower is only considered once). We replace these values in (24), and obtain C_b = 13,600 € per BS, which is further considered in (22).

Regarding C_{fi}, if there is channel of 5 MHz available within each cell, assuming that the annual cost of a license, for 3×5 MHz, is 82,500,000 € at 800 MHz, and 45,000,000 € at 2 GHz, both bands paired, for $K = 3$, and considering a total area of 91, 391.5 km^2 as the area of Portugal, the fixed cost per unit area is:

$$\begin{aligned} C_{fi\,800\,\text{MHz}[€/\text{km}^2]} &= \frac{82,500,000}{91,391.5 \times 5} = 180.542 \approx 180\,€/\text{km}^2 \\ C_{fi\,2\,\text{GHz}[€/\text{km}^2]} &= \frac{45,000,000}{91,391.5 \times 5} = 98.477 \approx 100\,€/\text{km}^2 \end{aligned} \tag{23}$$

A recapitulation of the costs is shown in Table 3. The revenue per cell per year, $(R_v)_{cell[€]}$, can be obtained as a function of the supported throughput per BS, $R_{b-sup[kbps]}$, and the revenue of a channel with data rate $R_{b[kbps]}$, $R_{b[€/min]}$, by:

$$(R_v)_{\text{cell}[€]} = \frac{N_{sec} \cdot R_{b-sup[\text{kbps}]} \cdot T_{bh} \cdot R_{R_{b[€/\text{min}]}}}{R_{b-ch[\text{kbps}]}} \tag{24}$$

where N_{sec} is the number of sectors, which in our case is 1 (using an omnidirectional antenna), T_{bh} is the equivalente duration of busy hours per day, and $R_{b-ch[\text{kbps}]}$ is the bit rate of the basic channel. T_{bh} considers only the active hours during a whole year, i.e., 6 h per working day expressed in minutes, then we have 6 busy hours per day, 240 busy days per year.

As in [12], we assume that project duration is of 5 years and there is a null discount rate; costs and revenues are taken on an annual basis. Although nowadays the trend is to consider flat rate for the revenues from data and multimedia traffic, in this work, one still considers the price per megabyte of information. We also consider a revenue/price of a 144 kbps channel per minute (approximately corresponding to the price of 1 MByte, as $144 \times 60 = 8,640\text{kb} \approx$ 1 MByte), $R_{144[€/\text{MByte}]}$. The revenue per cell can be obtained as:

Table 3 Assumptions for the costs with onminirectional BS antenna ($K = 3$)

Costs	Omnidirectional, $K = 3$
$C_{fi\,800\,\mathrm{MHz}[€/\mathrm{km}^2]}$	$180.542 \approx 180$
$C_{fi\,2\,\mathrm{GHz}[€/\mathrm{km}^2]}$	$98.477 \approx 100$
$C_{BS[€]}$	33,000
$C_{inst[€]}$	22,500
$C_{bh[€]}$	22,500
$C_{M\&O[€/\mathrm{year}]}$	1,500

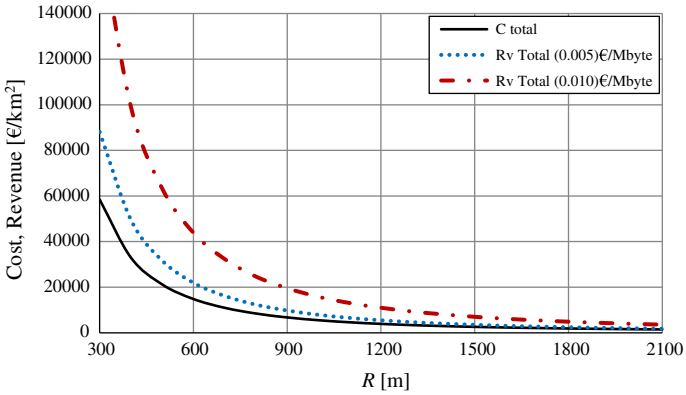

Fig. 10 Total cost and revenue versus R with different $R_{R_{b[€/min]}}$

$$(R_v)_{\mathrm{cell}[€]} = \frac{1 \cdot R_{b-sup[\mathrm{kbps}]} \cdot 60 \cdot 6 \cdot 240}{144_{[\mathrm{kbps}]}} \tag{25}$$

The (absolute) profit is given by:

$$P_{[€/\mathrm{km}^2]} = R_v - C \tag{26}$$

from which, the profit in percentage terms is given by:

$$P_{[\%]} = \frac{R_v - C}{C} \times 100 \tag{27}$$

In order to obtain profit optimization, revenues should be maximized with respect to cost. The revenue curves from Fig. 10 have been obtained for two values of $R_{144[€/\mathrm{MByte}]}$, i.e., 0.005 and 0.010 €/MByte (which corresponds to the price per MByte [13]). Figure 10 shows, as expected, that increasing the price per MByte, increases the revenue. The total cost is also presented and is lower than the revenues. One verifies that the curves for the cost and revenues are decreasing functions.

Figure 11 shows results for the profit in percentage as a function of cell radius, for different values of the price per MByte with CRRM and with the implemented iCRRM, comparing such profits with the profit from the simple system without applying SA. It is evident that the profit increases as the price per MByte increases; nevertheless, the curves keep the same shape and behaviour. By employing CRRM, when $R_{144[€/\mathrm{MByte}]} = 0.010$ €/MByte and $R = 1{,}000$ m, about 253 % profit is achieved, whilst a profit of 77 % has been obtained for $R_{144[€/\mathrm{MByte}]} = 0.005$ €/MByte. In turn, by employing iCRRM for the same cell radii, approximate profits of

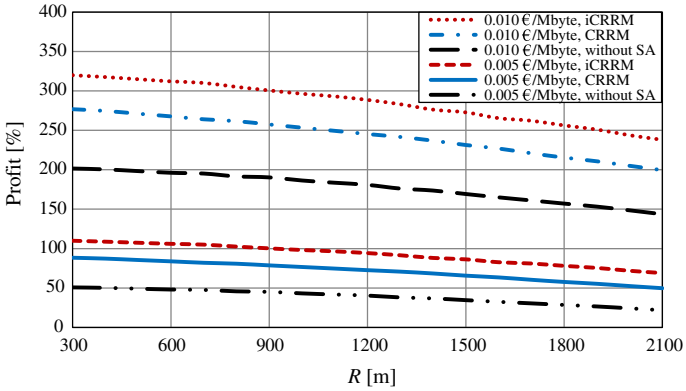

Fig. 11 Profit in percentage terms versus R with different $R_{R_{b[€/min]}}$ without SA, with CRRM and with iCRRM

296 and 98 % were obtained for price per MByte of 0.010 and 0.005 €, respectively. From the results it can be deducted that the profit decreases as the cell radius increases. However, this conclusion is somehow only valid under the assumption that there is an unlimited need for bandwidth and that users are willing to pay for it. Additionally, employing the basic CRRM allows for increasing the profit. However, with the use of iCRRM the improvement in the profit, in percentage terms, is considerably higher, as it is shown in Fig. 11.

7 Conclusions

This work proposes an innovative formulation to compute the average SINR in the context of SA in LTE systems, which comprises an iCRRM entity, presented in [3], and schedules the users between the two LTE systems operating at 800 MHz and 2 GHz, whilst considering the integer programming optimization and considering M-LWDF scheduler within each LTE system. Firstly, considering a topology with reuse pattern $K = 3$ and the COST-231 Hata model for the path loss, the average SINR in the cell was obtained. The values for the transmitter power have been found for different cell radii so that a constant average SINR could be kept.

From the analytical results, we have concluded that using the maximum average SINR is not recommended because the transmitter power would be extremely high. Instead, we have evaluated the transmitter power required to maintain a high average SINR (1, 5 and 10 % less than the maximum) for a value of orthogonality factor, $\alpha = 1$, and verified how the normalised power increases as the cell radius increases. For values of the average SINR lower than the maximum, the required transmitter power is reasonably lower than in the other cases ($V =$ 1 and 5 %).

The objective of the proposed multiband scheduler is to explore the integration of spectrum and network resource management functionalities in order to achieve higher performance and increase capacity gains in an IMT-A scenario. The performed simulations have shown a substantial improvement of the average cell throughput by employing SA enabling entities, e.g., a simpler CRRM and the iCRRM entity proposed in this work. Whereas results show that our normalised transmitter formulation approach enables to maintain an almost constant average throughput no matter the cell radii, it has also been shown that when 80 users are

considered, the achievable throughput is approximately 6,800, 8,500 and 9,500 kbps for the case without SA (in the presence of 80 simultaneous users within the cell, 40 for each 800 MHz and 2 GHz LTE system capacities), employing CRRM and employing iCRRM, respectively. Besides, in terms of average cell packet loss ratio, it was found that the CRRM and iCRRM present values of 11 and 7 %, respectively, whereas without SA, packet loss is 22 %. In the latter case, the average cell delay is equal to 32 ms while the application of both CRRM and iCRRM only presents a delay of 22 ms.

The dependence of the profit in percentage terms on the cell radius is analyzed for different values of the price, employing CRRM and also with the implemented iCRRM. Its value increases as the price per MByte increases. Nevertheless, the curves keep the same shape and behaviour. By employing CRRM, and with prices of 0.010 and 0.005 €/MByte, for R = 1,000 m, one obtains values for the profit, of 253 and 77 %, respectively. However, for the same cell radius, by employing iCRRM, as the achieved throughput is higher, respective values for the profit are higher, 296 and 98 %. From this analysis, it is possible to conclude that, although employing the basic CRRM allows for increasing the profit, to consider iCRRM enables to significantly enhance the profit in percentage terms. Future work includes addressing assumptions up to date on economic aspects, e.g., the equipment and installation costs, or princing models (e.g., flat fees).

Acknowledgements This work has been partially supported and funded by the FCT project PEst-OE/EEI/LA0008/2013, OPPORTUNISTIC-CR, LTE-Advanced Enhancements using Femtocells, CREaTION, COST IC0905 TERRA, COST IC 0902, COST IC 1004, by the Marie Curie Reintegration Grant PLANOPTI (FP7-PEOPLE -2009-RG), EFATraS, ECOOP, HANDCAD and ORCIP. The authors acknowledge the suggestions from Doctor Orlando Cabral and Prof. António Rodrigues. The authors also acknowledge colleagues from Viatel, who provided information on LTE costs, and Doctor Giuseppe Piro for his precious guidance in the implementation of spectrum aggregation functionalities into LTE-Sim.

References

1. Mihovska, A., Meucci, F., Prasad, N. R., Cabral, O., & Velez, F. J. (2009). Multi-operator resource sharing scenario in the context of IMT-advanced systems (invited paper). In *Proceedings of second international workshop on cognitive radio and advanced spectrum management (2009—CogART 2009), Aalborg, Denmark*.
2. The 3rd Generation Partnership Project (3GPP). www.3gpp.org
3. Cabral, O., Meucci, F., Mihovska, A., Velez, F. J., & Prasad, N. R. (2011). Integrated common radio resource management with spectrum aggregation over non-contiguous frequency bands. *Wireless Personal Communications*, *59*(3), 499–523.
4. Lee, H., Vahid, S., & Moessner, K. (2014). A survey of radio resource management for spectrum aggregation in LTE-advanced. *IEEE Communications Surveys Tutorials*, *16*(2), 745–760.
5. Piro, G., Grieco, L. A., Boggia, G., Capozzi, F., & Camarda, P. (2011). Simulating LTE cellular systems: An open source framework. *IEEE Transactions on Vehicular Technology*, *60*(2), 1–16.
6. 3GPP TR 25.892 v6.0.0. (2004). Feasibility study for orthogonal frequency division multiplexing (OFDM) for UTRAN enhancement. The 3rd Generation Partnership Project, Technical Specication Group Radio Access Network, June 2004.
7. Parsons, J. D., Turkmani, A. M. D., & Feng, J. (1989). The effect of base station antenna height on 900 MHz microcellular mobile radio systems. In *Proceedings of IEEE colloquium on microcellular mobile radio* (pp. 7/1–7/6). London: IET.
8. TS210371-Top signal full-band AWS/Cellular/LTE/PCS/WiMax omni-directional fiberglass antenna. www.wpsantennas.com
9. Holma, H., & Toskala, A. (Eds.). (2007). *WCDMA for UMTS HSPA evolution and LTE* (4th ed.). West Sussex, UK: Wiley.
10. Chen, K.-C., Roberto, J., & de Marca, B. (2008). *Mobile WiMAX* (1st ed.). West Sussex, UK: Wiley.
11. Salo, J., Nur-Alam, M., & Chang, K. (2010). Practical introduction to LTE radio planning. www.eceltd.com/lte_rf_wp_02Nov2010.pdf

12. Velez, F. J., Nazir, M. K., Prasad, R., Aghvami, H., Holland, O., & Robalo, D. (2010). Business models and cost/revenue performance. In R. Prasad & F. J. Velez (Eds.), *WiMAX networks: Techno-economic vision and challenges*. Dordrecht: Springer.
13. Velez, F. J., Anastácio, N., Merca, F., & Cabral, O. (2007). Cost/revenue optimization of multi-service cellular planning for business centre E-UMTS. In *Proceedings of IEEE 65th vehicular technology conference—VTC2007-Spring* (pp. 3194–3199).

Jessica Acevedo Flores electronics engineer from Universidad Catolica Santa Maria (Peru), is a M.Sc. In Networking and Computer Engineering from the National Taiwan University of Science and Technology (Taipei-Taiwan). She has been a fellow research for Instituto de Telecomunicações in Portugal for more than two years, participating in many conferences and seminars in Europe, as well as publishing few papers. Her academic interest mainly focuses in the telecommunications field: wireless networks (i.e. WiMAX, LTE, LTE-Advanced, WiFi), digital design and new electronic technologies. She has worked as an invited Professor in many universities in Peru, being invited as a lecturer in international congresses.

Daniel Robalo received the Licenciado and M.Sc. degrees in Electrical Engineering from University of Beira Interior (UBI), Covilhã, Portugal, in 2005 and 2008, respectively. He is currently a Ph.D. student at UBI and a researcher at *Instituto de Telecomunicações*, where he has been participating in several projects such as MobileMAN, Planopti, Ubiquimesh, OPPORTUNISTIC-CR, and CREaTION. His research interests include cellular planning and optimization, radio resource management, carrier aggregation, cost/revenue and energy trade-offs of mobile wireless communication systems.

Fernando J. Velez (M'93-SM'05) received the Licenciado, M.Sc. and Ph.D. degrees in Electrical and Computer Engineering from Instituto Superior Técnico, Technical University of Lisbon in 1993, 1996 and 2001, respectively. Since 1995 he has been with the Department of Electromechanical Engineering of Universidade da Beira Interior, Covilhã, Portugal, where he is Assistant Professor and he is also a researcher at Instituto de Telecomunicações. Fernando was a IEF Marie Curie Research Fellow in King's College London in 2008/09 (OPTIMOBILE IEF) and a Marie Curie ERG fellow at Universidade da Beira Interior from 2010 until March 2013 (PLANOPTI ERG). He made or makes part of the teams of RACE/MBS, ACTS/SAMBA, COST 259, COST 273, COST 290, IST-SEACORN, IST-UNITE, PLANOPTI, COST 2100, COST IC0902, COST IC0905 "TERRA', COST IC1004 and INSYSM European projects, he participated or is participating in SEMENTE, SMART-CLOTHING, UBIQUIMESH, NEUF (LTE-Advanced Enhancements using Femtocells), HANDCAD, ECOOP and CREaTION (Cognitive Radio Transceiver Design for Energy Efficient Data Transmission) Portuguese projects, and he was or is the coordinator of six Portuguese projects: SAMURAI, MULTIPLAN, CROSSNET, MobileMAN, OPPORTUNISTIC-CR and PROENERGY-WSN. Prof. Velez has been the coordinator of the WG2 (on Cognitive Radio/Software Defined Radio Coexistence Studies) of COST IC0905 "TERRA". Prof. Velez has authored two books, thirteen book chapters, 160 papers and communications in international journals and conferences, plus 30 in national conferences, is a senior member of IEEE, IT and Ordem dos Engenheiros (EUREL), and a member of IET. His main research areas are cellular planning tools, traffic from mobility, crosslayer design, spectrum sharing/aggregation, and cost/revenue performance of advanced mobile communication systems.